Formation and Structures of Transition Metal−C_{60} Clusters

Satoshi Nagao, Tsuyoshi Kurikawa, Ken Miyajima, Atsushi Nakajima, and Koji Kaya*

Department of Chemistry, Faculty of Science and Technology, Keio University, 3-14-1 Hiyoshi, Kohoku-ku, Yokohama 223, Japan

Received: February 12, 1998; In Final Form: April 6, 1998

Transition metal (Sc, Ti, V, and Cr)−C_{60} binary clusters were produced in the gas phase by a two-laser vaporization method. In the mass spectra of cationic $M_n(C_{60})_m^+$, for M = Sc, Ti, and V, clusters having the composition of $(n, m) = (1, 1)^+$, $(1, 2)^+$, $(2, 3)^+$, $(3, 4)^+$, $(4, 4)^+$, and $(5, 5)^+$ were predominantly produced. The peaks having $(n, n + 1)^+$ compositions are explicable in terms of multiple dumbbell structures, in which metal atoms and C_{60} are alternately stacked. Clusters with composition $(4, 4)^+$ and $(5, 5)^+$ are presumed to be ring structures. For $Cr_n(C_{60})_m^+$, however, a Cr atom is surrounded by three C_{60}, forming a tricapped structure, and the structure acts as a unit for larger stable clusters of $(2, 4)^+$, $(3, 4)^+$, and $(4, 4)^+$. Ionization energy measurements for neutral $M_n(C_{60})_m$ and a chemical probe method using CO, O_2, and C_2H_4 as reactants gave information concerning the geometrical and electronic structures.

1. Introduction

A laser vaporization method[1] has made it possible to vaporize metals having a high boiling temperature in a short time regime and to produce clusters consisting of hundreds of atoms. The application of laser vaporization to organometallic complexes consisting of transition metal atoms and organic molecules has been performed extensively in the gas phase, and several groups independently have succeeded in the synthesis of novel organometallic complexes.[2−7] Synthesis of organometallic compounds in the gas phase is valuable because (1) their properties can be investigated without the environmental influence of solvent and oxygen and (2) the preparation of metal atoms in electronic excited states is expected to open up new reaction pathways, producing novel compounds. For example, new organometallic compounds unknown in the bulk, such as V_n(benzene)$_m$ [8] and Co_n(benzene)$_m$,[9] have been recently discovered.

The investigation of fullerene-based organometallic compounds is intriguing because C_{60} acts as not only an electron donor but also an electron acceptor. This means that C_{60} can also form an ionic complex with alkali metals, alkaline earth metals, and lanthanides. These peculiar ligand properties of C_{60} make the studies of its derivatives attractive. Martin and co-workers have reported that a fullerene can be coated in the gas phase with layers of various metals[10,11] and that C_{60} can be linked by carbon atoms.[12] Complexes composed of a metal and a few fullerenes have been independently reported by the Freiser group and the Hercule group, who proposed a dumbbell structure for $M(C_{60})_2^+$ (M = Ni and Ag).[13,14] Furthermore, Duncan and co-workers have studied the photodissociation dynamics of Ag$(C_{60})_2^+$.[15]

Very recently, we have reported the production of vanadium (V)−C_{60} cluster cations ($V_n(C_{60})_m^+$) using the technique of two independent lasers for vaporization of solid rods of vanadium and C_{60}.[16] From the pattern of the abundant clusters in the mass spectrum and the reactivity toward O_2 and CO, it is concluded that the $V_n(C_{60})_{n+1}^+$ (n = 1−3) cluster cations take chain multiple dumbbell structures expressed by $V_n(\eta^6\text{-}C_{60})_{n+1}^+$, and $V_4(C_{60})_4^+$ takes a ring structure, with alternating V atoms and C_{60} molecules. Here, the superscript of the symbol η denotes how many carbon atoms in C_{60} are bonded to a metal atom.

We have successfully extended this method to other transition metals of Sc, Ti, and Cr, producing binary clusters between multi-transition metal atoms and multi-C_{60}, $M_n(C_{60})_m$ (M = Sc, Ti, V, and Cr). In particular, as published elsewhere,[17] the Co−C_{60} complexes exhibit a bonding feature different from that of V−C_{60}; a Co atom is tricapped by C_{60}, forming $Co(C_{60})_3$. In this article, we will discuss the difference in the bonding properties among them through the mass spectra, the reactivities toward CO, O_2, and C_2H_4, and ionization energies.

2. Experiments

Details of the experimental setup were previously described elsewhere.[16,17] Transition metal (M)−C_{60} binary clusters in the gas phase were produced by laser vaporization using the second harmonic of two pulsed Nd^{3+}:YAG lasers (wavelength = 532 nm). Each laser was focused onto a rotating and translating rod; one was a metal rod, and the other was a C_{60} rod. The second vaporization laser was fired with a ∼5 μs delay time after the first pulsed laser, which was adjusted to synchronize with the flow speed of the He carrier gas in order to mix them homogeneously. The fluence of the vaporization laser was 10−15 mJ/pulse for the transition metal rod and 70−100 μJ/pulse for the C_{60} rod. The vaporization of C_{60} was very sensitive to the laser fluence. For example, a laser fluence of more than 200 μJ/pulse resulted in noticeable "C_2 loss" fragmentation of C_{60}. Consequently, the laser vaporization of the C_{60} rod should occur downstream from that of the metal rod because the reverse order results in the fragmentation of C_{60} due to the high laser fluence for the metal rod. The hot vapors of metal and C_{60} were quenched to room temperature by a pulsed He carrier gas (5−6 atm stagnation pressure), and M−C_{60} clusters were generated. After the cluster beam was skimmed, the neutral clusters were ionized in a static electric field by an ArF excimer laser (6.42 eV) or the second harmonic of a dye laser pumped by an XeCl excimer laser, whereas the cluster cations were accelerated with a pulsed electric potential to +3 kV without photoionization. The ions were mass-analyzed by a time-of-flight (TOF) mass spectrometer with a reflectron. To detect

* To whom correspondence should be addressed.

S1089-5639(98)01136-0 CCC: $15.00
Published on Web 05/19/1998

heavy cluster ions efficiently, an ion detector known as an "Even-cup" was used[18] in which cations accelerated to 20 kV to hit a cup-like aluminum dynode and the ejected electrons extracted onto a grounded scintillator (NE102A, Oyokoken) were converted into photons that were detected by a photomultiplier (Hamamatsu, H6520).

To obtain information on the structure of $M-C_{60}$ clusters, the chemical probe of adsorption reactivity for the clusters was employed by use of the conventional flow-tube reactor.[19] Inside the flow-tube reactor, CO, O_2, C_2H_4, and C_6H_6 seeded in He was injected in synchronization with the flow of the clusters, and the adducts of $M-C_{60}$ clusters were also mass-analyzed.

In the ionization energy (E_i) measurement, the second harmonic of the dye laser was used as the ionization laser. The photon energy was changed at 0.01−0.03 eV intervals in the range of 5.92−5.0 eV, while the abundance and the composition of the clusters were monitored by the ionization of an ArF laser. The fluences of both the tunable ultraviolet (UV) laser and the ArF laser were kept at $\sim$200 μJ/cm^2 to avoid multiphoton processes. To obtain photoionization efficiency curves, the ion intensities of the mass spectra ionized by the tunable UV laser were plotted as a function of photon energy with the normalization to both the laser fluence and the ion intensities of ArF ionization mass spectra. The E_i's of the clusters were determined from the final decline of the photoionization efficiency curves. The uncertainties of the E_i's were estimated to be typically $\pm$0.05 eV.

3. Results and Discussion

3.1. Structures of Sc−C_{60}, Ti−C_{60}, and V−C_{60} Clusters. Figure 1 shows TOF mass spectra of $M_n(C_{60})_m^+$ (M = (a) Sc, (b) Ti, and (c) V) cluster cations. Peaks of the cationic clusters are labeled according to the notation, $(n, m)^+$, denoting the number of metal atoms (n) and C_{60} (m). Under this condition, the contribution of M_n^+ cluster to $M_n(C_{60})_m^+$ formation was negligible because the abundance of the M_n^+ clusters ($n \geq 2$) was less than $^1/_{100}$ compared with that of the M^+ atom. The mass spectrum of $Ti_n(C_{60})_m^+$ was obtained with a higher laser fluence of vaporization compared with the others. As a result, the clusters having rich metal atoms were formed abundantly. These TOF mass spectra indicate three common features. (i) The main products are $(1, 2)^+$, $(2, 3)^+$, $(3, 4)^+$, $(4, 4)^+$, and $(5, 5)^+$. (ii) The $(4, 4)^+$ product is more abundant than $(3, 4)^+$, while $(5, 4)^+$ is less abundant than $(4, 4)^+$. (iii) The $(4, 5)^+$ product is scarcely produced; instead $(5, 5)^+$ is the first prominent peak in the $(n, 5)^+$ series.

To deduce the structure of the $M-C_{60}$ clusters by the chemical probe method, the reactivity of these abundant clusters toward O_2 gas was measured. Figure 2 shows mass spectra of $Ti_n(C_{60})_m^+$ before and after the oxidation reaction. The abundant clusters with $(n, m) = (1, 2)^+$, $(2, 3)^+$, $(3, 4)^+$, $(4, 4)^+$, and $(5, 5)^+$ were nonreactive toward O_2, whereas the other species drastically diminished with the injection of O_2 followed by O-atom adducts formation ($Ti_n(C_{60})_mO_k^+$). It is reasonably presumed that an exterior Ti atom in $Ti_n(C_{60})_m^+$ is a reaction site for the oxidation because C_{60}^+ itself does not show the oxidation reaction. Namely, these results indicate that the Ti−C_{60} clusters of $(1, 2)^+$, $(2, 3)^+$, $(3, 4)^+$, $(4, 4)^+$, and $(5, 5)^+$ have no exterior Ti atoms. As well as the Ti−C_{60} clusters, the abundant species of the Sc−C_{60} clusters also show no reactivity toward O_2. As reported previously for $V_n(C_{60})_m^+$, the presumed geometry of $(n, n + 1)^+$ at $n = 1-3$ is a multiple dumbbell structure (parts a−c of Figure 3) and that of $(n, n)^+$ at $n = 4$ or 5 is a ring structure (parts d and e of Figure 3) on the basis of

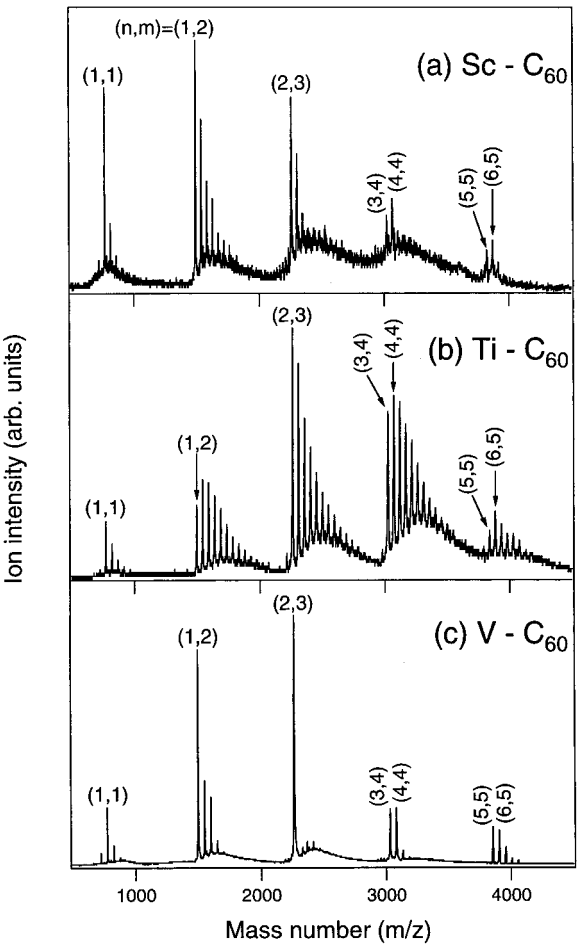

Figure 1. TOF mass spectra of transition metal (M = Sc, Ti, and V)−C_{60} cations, $M_n(C_{60})_m^+$: (a) $Sc_n(C_{60})_m^+$; (b) $Ti_n(C_{60})_m^+$; (c) $V_n(C_{60})_m^+$. Peaks of the clusters are labeled according to the notation (n, m), denoting the number of metal atoms (n) and C_{60} molecules (m).

no reactivities toward O_2 or CO gas,[16] where the V atom and C_{60} are alternately stacked. Both the striking similarities among the three TOF mass spectra in Figure 1 and their reactivity toward O_2 suggest that not only $V_n(C_{60})_m^+$ but also $Sc_n(C_{60})_m^+$ and $Ti_n(C_{60})_m^+$ clusters take the chainlike multiple dumbbell structure or the ring structure. As shown in Figure 2, there is no necessity for linear chain structures of $(n, n + 1)^+$ at $n = 2$ and 3 because C_{60} consists of many rings for bonding sites; there are 12 pentagonal rings and 20 hexagonal rings. As shown in Figure 3e, moreover, there may be two plausible structures for (5, 5), which are the ring of (4, 4) branching out (1, 1) and a monocyclic ring, although we cannot decide between them.

By the use of an ArF laser, we obtained the TOF mass spectra of neutral $M_n(C_{60})_m$ clusters whose features are identical with those of $M_n(C_{60})_m^+$ cluster cations. Then it is reasonably presumed that $(n, m) = (1, 2)$, $(2, 3)$, $(3, 4)$, $(4, 4)$, and $(5, 5)$ for neutral $M_n(C_{60})_m$ clusters, which also have the dumbbell or the ring structures. Experimentally, it was relatively difficult to obtain the mass spectra of the neutral $M_n(C_{60})_m$ clusters by photoionization compared with those of the $M_n(C_{60})_m^+$ cluster cations because of their low ionization efficiencies. This is probably because their ionization energy is close to the photon energy of the ArF laser (6.42 eV), which will be discussed below in section 3.4.

3.2. Reactivity of $M_n(C_{60})_m^+$ (M = Sc, Ti, and V) Cluster Cations toward CO. To investigate the metal−C_{60} bonding in the dumbbell clusters, the examination of reactivity of $M_n(C_{60})_m^+$ (M = Sc, Ti, and V) toward CO gas was performed.

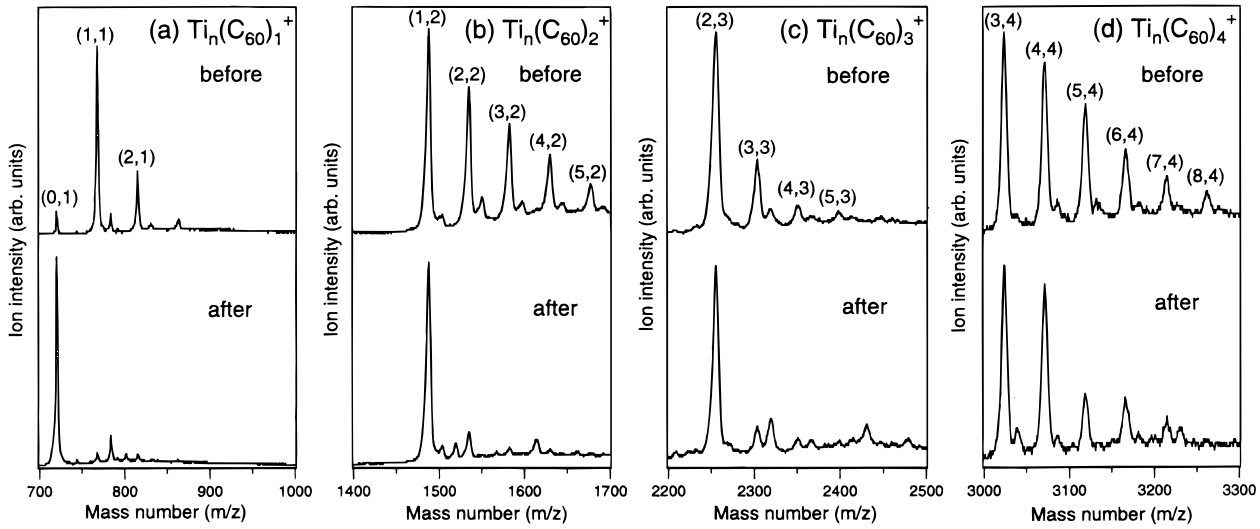

Figure 2. Expanded view of time-of-flight mass spectra before (top) and after (bottom) oxidation reactions: (a) $Ti_n(C_{60})_1^+$; (b) $Ti_n(C_{60})_2^+$; (c) $Ti_n(C_{60})_3^+$; (d) $Ti_n(C_{60})_4^+$.

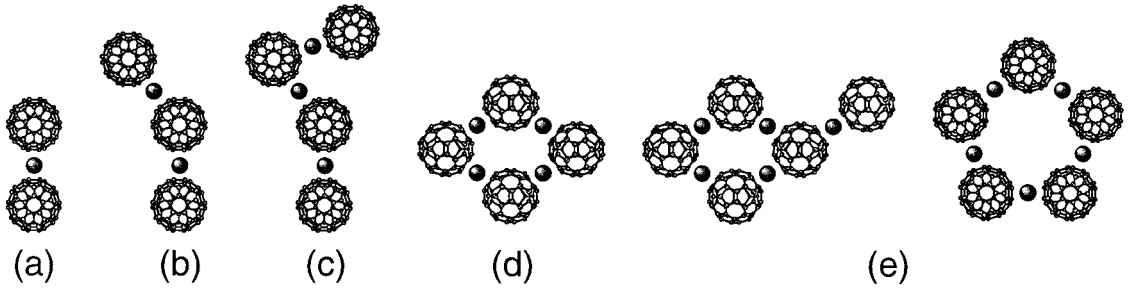

Figure 3. Proposed geometric structures of (a) $M_1(C_{60})_2^+$, (b) $M_2(C_{60})_3^+$, (c) $M_3(C_{60})_4^+$, (d) $M_4(C_{60})_4^+$, and (e) $M_5(C_{60})_5^+$ (M = Sc, Ti, and V).

Since CO can generally be regarded as a two-electron donor, the determination of the maximum number of CO adsorbed (k_{max}) enables us to apply electron counting to the complexes. The metal atom in $M_n(C_{60})_m^+$ is a reaction site for CO because C_{60}^+ itself is inert for CO as well as O_2. The reactivity measurement indicates that the abundant dumbbell/ring clusters were nonreactive, whereas the other $M_n(C_{60})_m^+$ clusters reacted with CO, forming carbonyl complexes. Figure 4 shows mass spectra of $Sc_n(C_{60})_1^+$, before and after the reaction with CO. $Sc_1(C_{60})_1^+$ clearly decreases, while $Sc_1(C_{60})_1(CO)_4^+$ newly appears. Even with a higher concentration of CO, $Sc_1(C_{60})_1(CO)_4^+$ is produced as a final product of $Sc_1(C_{60})_1^+$, and therefore, k_{max} is 4 for $Sc_1(C_{60})_1^+$. On the other hand, as shown in Figure 5, $Ti_1(C_{60})_1^+$ and $V_1(C_{60})_1^+$ resulted in $Ti_1(C_{60})_1(CO)_3^+$ and $V_1(C_{60})_1(CO)_3^+$, respectively, and their k_{max} is 3.

For organometallic complexes, the 18-electron rule is useful for discussing their electronic stability qualitatively.[20] Armentrout and co-workers have reported that $V(CO)_n^+$ and $Ti(CO)_n^+$ are formed up to $n = 7$, satisfying the 18-electron rule strictly. However, the dissociation energies of $V(CO)_{n-1}^+$−CO and those of $Ti(CO)_{n-1}^+$−CO at $n = 7$ are about half of those at $n =$ 4−6, suggesting that the satisfaction of 16 valence electrons (VEs) can make the clusters stable toward the CO addition.[21,22] On a MO diagram under C_{6v} or D_{6h} symmetry, indeed, the 9th orbital, which is filled by the 17th and 18th electrons, has nonbonding character, leading to less electronic stabilization.[23] In fact, almost no $Ti(CO)_7^+$ and $V(CO)_7^+$ were observed under our conditions, while $Ti(CO)_6^+$ and $V(CO)_6^+$ were abundantly produced.[24] The total numbers of VEs of $Ti(CO)_6^+$ and $V(CO)_6^+$ are 15 and 16, respectively, so the criterion of 16 VEs seems able to explain the electronic structure after CO adsorption.

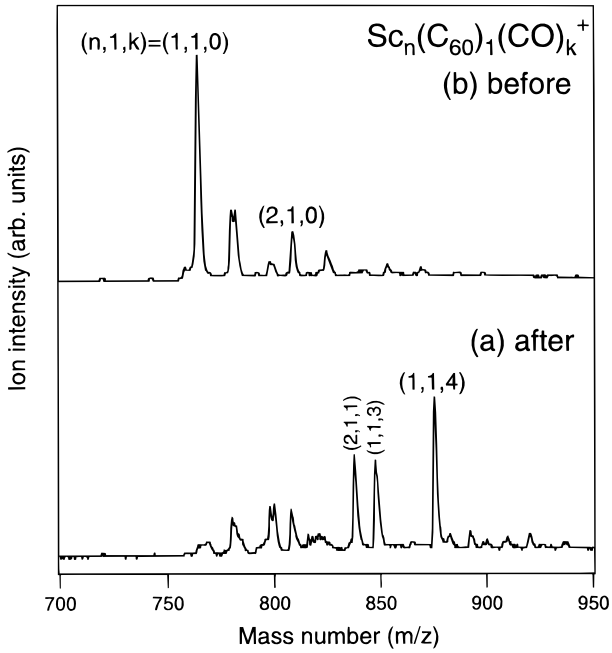

Figure 4. TOF mass spectra of $Sc_n(C_{60})_1(CO)_k^+$ (a) after and (b) before the reaction with CO gas. Peaks of the clusters are labeled according to the notation (n, 1, k), denoting the number of Sc atoms (n) and CO molecules (k).

As shown in Figures 4 and 5, $M_1(C_{60})_1^+$ can bond four CO for Sc ($k_{max} = 4$) and three CO for M = Ti and V ($k_{max} = 3$). Assuming that C_{60} acts as an η^6-ligand, $Sc_1(C_{60})_1(CO)_4^+$ has 16 VEs, whereas $M_1(C_{60})_1(CO)_3^+$ has 15 (16) VEs for M = Ti (V). If C_{60} behaves as an η^5-ligand, $Ti_1(C_{60})_1(CO)_3^+$ having 14 VEs should react with one more CO to satisfy the 16 VEs.

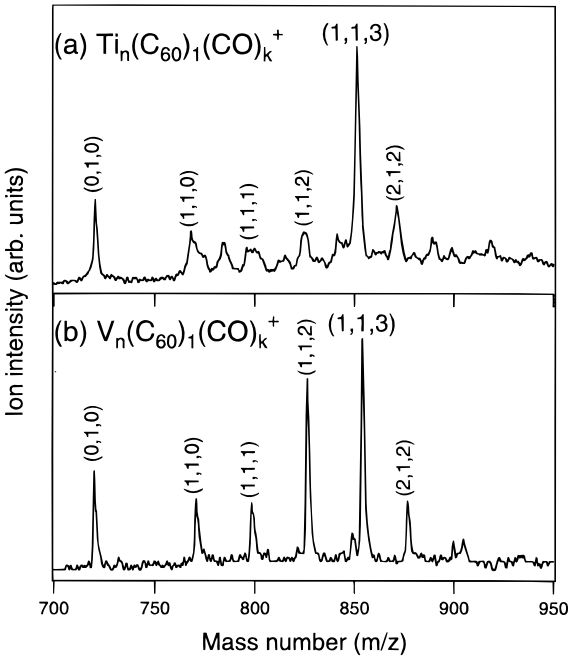

Figure 5. TOF mass spectra of (a) $Ti_n(C_{60})_1(CO)_k^+$ and (b) $V_n(C_{60})_1(CO)_k^+$ after reaction with CO gas.

Furthermore, since the metal−benzene complex of $M(C_6H_6)_1^+$ take the same number of k_{max} toward CO as $M_1(C_{60})_1^+$,[24] it is safely concluded that C_{60} acts as an η^6-ligand for Sc, Ti, and V.

On the other hand, $M_1(C_{60})_2^+$ has 14, 15, and 16 VEs for M = Sc, Ti, and V, respectively. According to the criterion of 16 VEs, $Sc_1(C_{60})_2^+$ can take one CO, but it shows no reactivity as described above. This is probably because the steric hindrance of C_{60} avoids reaction with CO. In fact, $Sc(C_6H_6)_2^+$ is similarly nonreactive toward CO and O_2. In summary, in both $M(C_{60})_1^+$ and $M(C_{60})_2^+$ (M = Sc, Ti, and V), C_{60} bonds the metal atom at a hexagonal ring: $M(\eta^6\text{-}C_{60})_1^+$ and $M(\eta^6\text{-}C_{60})_2^+$. Furthermore, it is reasonable to extend this bonding scheme to that of the other dumbbell clusters. They can be expressed as $Sc_n(\eta^6\text{-}C_{60})_m^+$, $Ti_n(\eta^6\text{-}C_{60})_m^+$, and $V_n(\eta^6\text{-}C_{60})_m^+$. This conclusion about the binding site is rationalized again by measurement of the ionization energy, as described below.

It should be noted that a bare Sc^+ atom itself is nonreactive toward CO, while its C_{60} or C_6H_6 complex is reactive. The carbonyl complex of $Sc(CO)_n^+$ has never been reported, and we could not observe it in our experiment,[24] in contrast to $Ti(CO)_n^+$ and $V(CO)_n^+$. Although the Sc atom is classified as an early transition metal, its properties are different from others in the electronic configuration. The larger radial extent of the metal valence s orbital leads to large metal−ligand repulsion and hence longer bond lengths. The effect results in the ground states of metal−ligand complex being derived from the excited states $3d^{n+1}$ asymptotes of the metal. Thus, M^+ promotes an s electron to the d orbital to enhance bonding, from $4s^23d^n$ to $4s^13d^{n+1}$. For Sc^+, however, it is relatively difficult to promote to the $3d^{n+1}$ occupation because of the large energy separation between the ground and excited states. Thus, the bonding between an Sc atom and ligands often has an ionic character rather than a covalent character, in contrast to Ti and V. In the formation of an M−ligand complex, generally, early transition metal prefers a π-donor ligand such as C_6H_6, while late transition metals prefer a π-acceptor ligand such as CO, depending on the number of d electrons it has. Especially for Sc, therefore, the π-donor ligand is so indispensable for overcoming the large energy separation that Sc never bonds to CO without the π-donor ligands. Thus, an Sc atom can bond to CO after it attaches to a complex with the π-donor ligand, as seen in $Sc_1(C_{60})_1(CO)_4^+$.

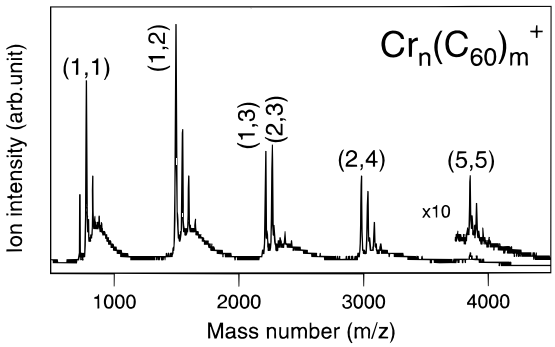

Figure 6. Time-of-flight mass spectrum of $Cr_n(C_{60})_m^+$. Peaks of the clusters are labeled according to the notation (n, m), denoting the number of Cr atoms (n) and C_{60} molecules (m).

3.3. Mass Spectra and Structures of Cr−C_{60} Clusters. Figure 6 shows a TOF mass spectrum of $Cr_n(C_{60})_m^+$, where Cr is located at the right of V in the periodic table. The main products of $Cr_n(C_{60})_m^+$ were $(n, m) = (1, 1)^+$, $(1, 2)^+$, $(1, 3)^+$, $(2, 4)^+$, and $(5, 5)^+$ for $m = 1-5$. This pattern is apparently different from that of $Sc_n(C_{60})_m^+$, $Ti_n(C_{60})_m^+$, and $V_n(C_{60})_m^+$. For $Cr_n(C_{60})_m^+$, $(1, 3)^+$ and $(2, 4)^+$ newly appeared as prominent peaks. To deduce the geometric structure, the reactivity of the $Cr_n(C_{60})_m^+$ clusters toward O_2, ethylene (C_2H_4), and C_6H_6 was investigated. For Cr−C_{60}, these reactants show similar reactivity for their adduct formation, although the reaction toward O_2 was accompanied by fragmentation to C_{60}^+. Figure 7 shows mass spectra of $Cr_n(C_{60})_m^+$ ($m = 1-3$) exposed to ethylene with different concentrations, although the difference in the concentration is qualitative. Figure 7a shows the distribution of $Cr_n(C_{60})_m^+$ ($m = 1-3$) before the ethylene reaction. At low concentration of ethylene (Figure 7b), only $(1, 1)^+$ easily forms the adduct of $(1, 1)^+-C_2H_4$, whereas the others are almost nonreactive. Since the Cr atom in $(1, 1)^+$ is distinctly exposed as an exterior atom, it is easy for C_2H_4 to react. With increasing concentration of C_2H_4, most of the $Cr_n(C_{60})_m^+$ forms the adduct. Even with the high concentration of C_2H_4 (Figure 7d), however, only $(1, 3)^+$ remains nonreactive, indicating that the Cr atom is blocked by three C_{60}. As demonstrated by $M_n(C_{60})_{n+1}^+$ (M = Sc, Ti, and V) in the preceding sections, the dumbbell structure should lead to inertness of $(n, n + 1)^+$ toward the reactant gas, but $(1, 2)^+$ and $(2, 3)^+$ for Cr−C_{60} exhibit the adduct formation as shown in parts c and d of Figure 7. This result indicates that they can afford the reactant gas to attach to the Cr atom(s). Then the most plausible structure for $(1, 2)^+$ is a bent structure, as shown in Figure 8a, where there is room for the reactant to adsorb. Since the reactivity of $(1, 2)^+$ and $(2, 3)^+$ is less than those of other $(n, m)^+$ ($n > m$) having more metal atoms, it is actually suggested that the Cr atom sandwiched by C_{60} is partially exposed in $(1, 2)^+$ and $(2, 3)^+$.

The $(n, 4)^+$ series $(2, 4)^+$, $(3, 4)^+$, and $(4, 4)^+$, as well as $(1, 3)^+$, are also nonreactive toward ethylene even with the high concentrations, while $(5, 4)^+$ and $(6, 4)^+$ were reactive. These four species are also nonreactive toward the other reactant gases of O_2 and C_6H_6. Since an exterior Cr atom should react with the reactant as discussed above, this result of the inertness is attributed to the fact that $(2, 4)^+$, $(3, 4)^+$, and $(4, 4)^+$ have no exterior Cr atom in the clusters, although the inert reactivity does not directly offer any conclusion about the position of the metal atoms, i.e., whether the atoms are isolated by C_{60} or cluster

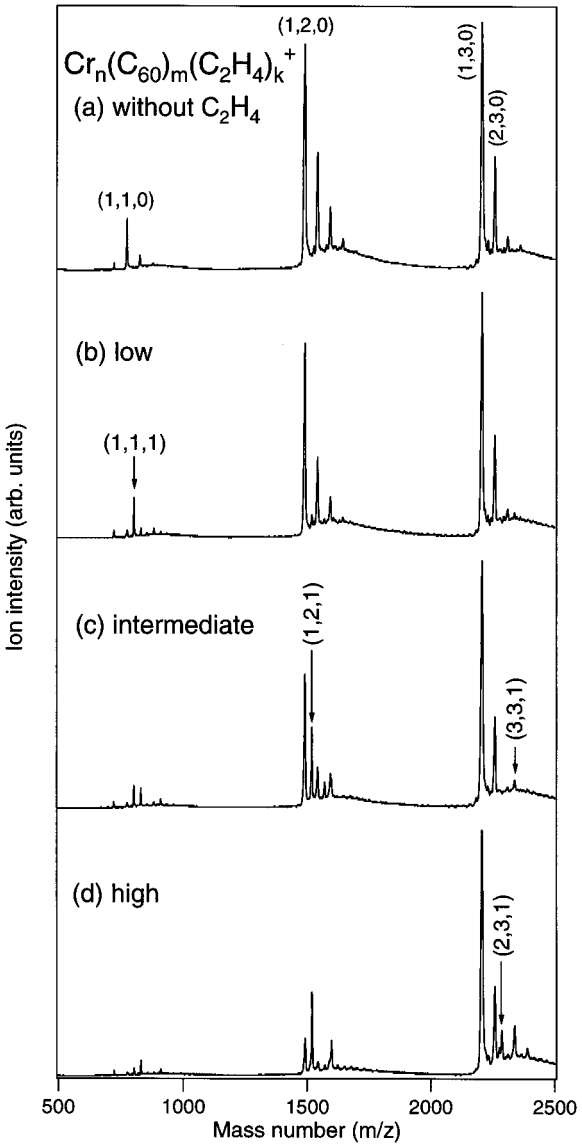

Figure 7. TOF mass spectra of $Cr_n(C_{60})_m^+$ reacted at different pressures of ethylene (C_2H_4) gas: (a) without ethylene; (b) with ethylene at low pressure; (c) at intermediate pressure; (d) at high pressure. Peaks of the clusters are labeled according to the notations (*n*, *m*, *k*), denoting the number of Cr atoms (*n*), C_{60} molecules (*m*), and C_2H_4 molecules (*k*), respectively.

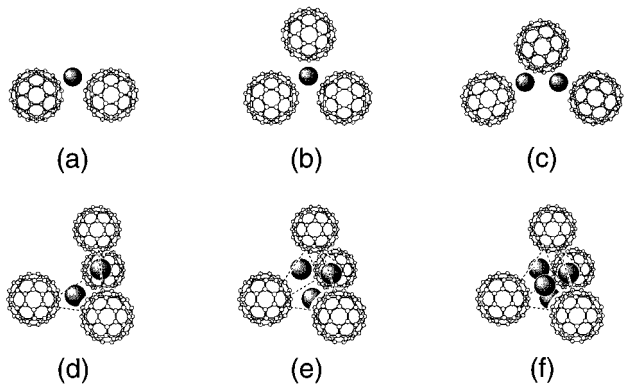

Figure 8. Proposed geometric structures of (a) $Cr_1(C_{60})_2^+$, (b) $Cr_1(C_{60})_3^+$, (c) $Cr_2(C_{60})_3^+$, (d) $Cr_2(C_{60})_4^+$, (e) $Cr_3(C_{60})_4^+$, and (f) $Cr_4(C_{60})_4^+$.

with each other. Since the compositions of the stable species in the $(n, 4)^+$ series are the same as those of Co−C_{60},[17] the plausible structures of $(2, 4)^+$, $(3, 4)^+$, and $(4, 4)^+$ can be presumed to be similar to those of Co−C_{60}, as shown in parts d−f of Figure 8. In them, the tricapped $Cr(C_{60})_3$ acts as a unit to form an $(n, 4)^+$ series. For $(2, 4)^+$, the first Cr atom surrounded by three C_{60} forms the stable $Cr(C_{60})_3$, and then the second Cr atom forms another local $Cr(C_{60})_3$ using the fourth C_{60}, which results in a double tricapped plane of $(2, 4)^+$. For $(3, 4)^+$ and $(4, 4)^+$, the third and the fourth Cr atoms form additional local $Cr(C_{60})_3$ groups, resulting in the trigonal pyramid. In $(4, 4)^+$, therefore, two tetrahedra (trigonal pyramids) of Cr_4 and $(C_{60})_4$ form a "face-centered tetrahedral structure" without bonds between Cr atoms.

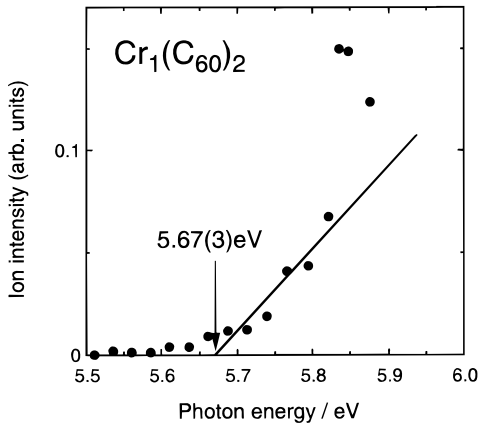

Figure 9. Photoionization efficiency (PIE) curve for $Cr_1(C_{60})_2$. The E_i of the cluster was determined to be 5.67 ± 0.03 eV from the final decline of the PIE curve.

Thus, $(1, 3)^+$ takes a tricapped planar structure in which the Cr atom is surrounded by three C_{60} (Figure 8b). The stable $(1, 3)^+$ cluster is generally observed in the late transition metal−C_{60} complexes, such as Fe−C_{60},[25] Co−C_{60},[17] and Ni−C_{60}.[25] Namely, there is distinction between V and Cr of whether the metal atom is bicapped or tricapped by C_{60}. If C_{60} behaves only as the η^6-ligand, the Cr atom should result in the stable structure of a bicapped dumbbell similar to the bis(benzene)-chromium molecule, $Cr(C_6H_6)_2$, which satisfies the 18-electron rule. On the basis of the 18-electron rule, the formation of $Cr(C_{60})_3^+$ indicates that not all of the C_{60} in it acts as the η^6-ligand. As pointed out elsewhere,[17] C_{60} is able to act as an η^3-ligand in Co−C_{60}. Then the most probable structure is $Cr(\eta^6\text{-}C_{60})_1(\eta^3\text{-}C_{60})_2$, which satisfies the 18-electron rule; the three C_{60} are not equivalent. In fact, the ligand of η^6-C_{60} is suggested by low ionization energy of (1, 3), as described below.

From a comparison of Cr−C_{60} with Co−C_{60}, the mass distributions are different, especially at $(2, 3)^+$. $(2, 3)^+$ for Cr−C_{60} has enough intensity to be detected, while $(2, 3)^+$ for Co−C_{60} is very weak and $(n, 3)^+$ are scarcely produced at $n \geq 2$.[17] This difference indicates that the chainlike structure might contribute to form stable $Cr_2(C_{60})_3^+$ (Figure 8c). For the C_{60} complex of early transition metals, a linear chain or a ring structure is preferable, whereas for late transition metals a three-dimensional lump structure becomes preferable. Cr is located at the border between early and late transition metals so that Cr−C_{60} seemingly takes the chainlike structures as well as the lump structures.

3.4. Ionization Energies of $M_1(C_{60})_m$ and $M_1(C_{60})_m(C_6H_6)_k$ (M = Sc, Ti, V, and Cr). The ionization energies (E_is) of neutral $M_1(C_{60})_m$ clusters ($m = 1-3$; M = Sc, Ti, V, and Cr) and their benzene complexes were determined by a photoionization spectroscopic method. Figure 9 shows the photoionization efficiency (PIE) curve for $Cr_1(C_{60})_2$. The E_i of $Cr_1(C_{60})_2$ was determined to be 5.67 ± 0.03 eV from the final decline of the PIE curve. In addition to this value, the E_is of the other

TABLE 1: Ionization Energy (E_i) of $M_n(C_{60})_m(C_6H_6)_k$ Clusters (M = Sc, Ti, V, and Cr) in eV[a]

cluster	ionization energy			
	M = Sc	M = Ti	M = V[b]	M = Cr
$M_1(C_{60})_1$	5.92−6.42	5.92−6.42	5.92−6.42	5.92−6.42
$M_1(C_{60})_2$	5.75(5)	5.93(5)	5.82(5)	5.67(3)
$M_1(C_{60})_3$				5.71(5)
$M_1(C_{60})_1(C_6H_6)_1$	5.54(3)	5.90(5)	5.61(3)	5.71(3)
$M_1(C_6H_6)_2$	5.05(5)	5.68(4)	5.75(3)	5.43(2)

[a] Values in parentheses represent the error times 10^{-2}. For example, 5.75(5) represents 5.75 ± 0.05. [b] Reference 16.

species are tabulated in Table 1. These E_is are vertical ionization thresholds rather than adiabatic ones because a Franck−Condon shift in the E_is might be expected in the production of the cations, where the charge would be distributed mainly on a metal atom. The E_is of $Sc_1(C_{60})_1(C_6H_6)_1$, $V_1(C_{60})_1(C_6H_6)_1$, $Cr_1(C_{60})_2$, and $Cr_1(C_{60})_1(C_6H_6)_1$ were determined from the final decline of the PIE curves, although the others were determined from their appearance photon energy because it was difficult to obtain the PIE curve for them being close to the limit of tunable range of the UV laser. The E_is for all of the $M_1(C_{60})_1$ were higher than 5.92 eV and lower than 6.42 eV because these clusters cannot be photoionized by the UV photon of 209.5 nm but can be done by the ArF laser.

All the E_i values of the tabulated clusters are lower than those of the metal atoms (Sc, 6.54 eV; Ti, 6,82 eV; V, 6.74 eV; Cr, 6.76 eV), C_{60} (7.61 eV), and C_6H_6 (9.24 eV). Moreover, the E_i of the $M_1(C_6H_6)_2$ is similar to those of $M_1(C_{60})_1(C_6H_6)_1$ and $M_1(C_{60})_2$. The similarity in E_is of $M_1(C_{60})_x(C_6H_6)_y$ $(x + y = 2)$ evidently shows that the metal atom is sandwiched between the six-membered rings of C_{60} rather than the five-membered rings. In fact, E_i becomes much higher in a bis(cyclopentadienyl) complex (for example, $V_1(C_5H_5)_2$; $E_i = 6.78$ eV), where the M atom is sandwiched between the five-membered rings. It can be generally seen that the interaction with η^6-C_{60} results in a relatively low E_i of 5.5−5.7 eV. This conclusion is consistent with the result from the reactivity of the clusters in the chemical probe experiment.

As reported elsewhere,[8,26] the E_i value of the $M_n(C_6H_6)_{n+1}$ sandwich cluster decreases greatly with the number n, the E_is of $V_n(C_6H_6)_{n+1}$ being 5.75, 4.70, 4.14, and 3.83 eV for $n = 1$, 2, 3, and 4, respectively. However, the E_i value of the $M_n(C_{60})_{n+1}$ dumbbell cluster never decreases with the cluster size. The reason is probably attributed to the difference in the interaction between d electrons of the metal atom and the π electron of the carbon ring; the d−π interaction is discontinuous in $M_n(C_{60})_m$, while it is continuous in $M_n(C_6H_6)_m$ along a molecular axis.

For Cr−C_{60}, the E_i of the tricapped $Cr_1(C_{60})_3$ is similar to those of the bicapped $M(C_{60})_2$ (M = Sc, Ti, V, and Cr). The E_i of $Cr_1(C_{60})_3$ presents a great contrast to those of other $M_1(C_{60})_3$ (M = Fe, Co, and Ni); all the E_is of $Fe_1(C_{60})_3$, $Co_1(C_{60})_3$, and $Ni_1(C_{60})_3$ are above 6.42 eV.[17,25] As discussed previously, C_{60} acts as an η^3-ligand in $Co(C_{60})_3$.[17] Then the low E_i of $Cr_1(C_{60})_3$ (5.71 eV) is reasonable if one of the C_{60} acts as the η^6-ligand in $Cr_1(C_{60})_3$, which was pointed out in the preceding section. This fact implies that the d−π interaction at the η^6-ligand should result in a larger stabilization in a cationic state compared with that in a neutral state.

4. Conclusions

In the gas phase, transition metal (M = Sc, Ti, V, and Cr)−C_{60} binary cluster cations, $M_n(C_{60})_m^+$, were produced by a two-laser vaporization method. From the pattern of the predominant peaks in the mass spectra, the most abundant clusters for M = Sc, Ti, and V were $(n, n + 1)^+$, the multiple dumbbell clusters. From the reactivity of the dumbbell clusters toward CO, it was concluded that they could be expressed as $Sc_n(\eta^6\text{-}C_{60})_m^+$, $Ti_n(\eta^6\text{-}C_{60})_m^+$, and $V_n(\eta^6\text{-}C_{60})_m^+$. In contrast, for M = Cr, the clusters of $(n, m) = (1, 2)^+$, $(1, 3)^+$, $(2, 4)^+$, and $(5, 5)^+$ were abundant. From the reactivity toward C_2H_4, $(1, 3)^+$, $(2, 4)^+$, $(3, 4)^+$, and $(4, 4)^+$ of Cr−C_{60} species have no exterior Cr atom, and it was deduced that $Cr_1(C_{60})_3^+$ forms the tricapped structure, and $(2, 4)^+$, $(3, 4)^+$, and $(4, 4)^+$ consist of the (1, 3) units. The most plausible structure for $Cr_4(C_{60})_4^+$ is a face-centered tetrahedron. From the ionization energies of $M_1(C_{60})_1$, $M_1(C_{60})_2$, $M_1(C_{60})_1(C_6H_6)_1$, and $M_1(C_{60})_3$ clusters, it is suggested that the M−C_{60} bonding in these clusters arises from the interaction between d electrons of the metal atom and π electrons of the hexagonal carbon ring (η^6).

Acknowledgment. This work is supported by a Grant-in-Aid for Scientific Research on Priority Areas from the Ministry of Education, Science, Sports, and Culture. A.N. expresses his gratitude to the Ishikawa Carbon Science Foundation for partial financial support. T.K. expresses his gratitude to research fellowships of the Japan Society for the Promotion of Science for Young Scientists.

References and Notes

(1) Rohlfing, E. A.; Cox, D. M.; Kaldor, A. *J. Chem. Phys.* **1984**, *81*, 3322.
(2) Teh, C. S.; Willey, K. F.; Robbins, D. L.; Pilgrim, J. S.; Duncan, M. A. *Chem. Phys. Lett.* **1992**, *196*, 233.
(3) Higashide, H.; Kaya, T.; Kobayashi, M.; Shinohara, H.; Sato, H. *Chem. Phys. Lett.* **1990**, *171*, 297.
(4) Holland, P. M.; Castleman, A. W., Jr. *J. Chem. Phys.* **1982**, *76*, 4195.
(5) Robels, E. S. J.; Ellis, A. M.; Miller, T. A. *J. Chem. Phys.* **1992**, *96*, 8791.
(6) Misaizu, F.; Sanekata, M.; Fuke, K.; Iwata, S. *J. Chem. Phys.* **1994,** *100*, 1161.
(7) Mitchell, S. A.; Blits, M. A.; Siegbahn, P. E. M.; Svensson, M. *J. Chem. Phys.* **1994**, *100*, 423.
(8) Hoshino, K.; Kurikawa, T.; Takeda, H.; Nakajima, A.; Kaya, K. *J. Phys. Chem.* **1995**, *99*, 3053.
(9) Kurikawa, T.; Hirano, M.; Takeda, H.; Yagi, K.; Hoshino, K.; Nakajima, A.; Kaya, K. *J. Phys. Chem.* **1995**, *99*, 16248.
(10) Zimmermann, U.; Malinowski, N.; Burkhardt, A.; Martin, T. P. *Carbon* **1995**, *33*, 995.
(11) Tast, F.; Malinowski, N.; Frank, S.; Heinebrodt, M.; Billas, I. M. L.; Martin, T. P. *Phys. Rev. Lett.* **1996**, *77*, 3529.
(12) Tast, F.; Malinowski, N.; Billas, I. M. L.; Heinebrodt, M.; Branz, W.; Martin, T. P. *J. Chem. Phys.* **1997**, *107*, 6980.
(13) Huang, Y.; Freiser, B. S. *J. Am. Chem. Soc.* **1991**, *113*, 8186.
(14) Zimmerman, P. A.; Hercules, D. M. *Appl. Spectrosc.* **1993**, *47*, 1545.
(15) Reddic, J. E.; Robinson, J. C.; Duncan, M. A. *Chem. Phys. Lett.* **1997**, *279*, 203.
(16) Nakajima, A.; Nagao, S.; Takeda, H.; Kurikawa, T.; Kaya, K. *J. Chem. Phys.* **1997**, *107*, 6491.
(17) Kurikawa, T.; Nagao, S.; Miyajima, K.; Nakajima, A.; Kaya, K. *J. Phys. Chem. A* **1998**, *102*, 1743.
(18) Harberland, H. *Clusters of Atoms and Molecules*; Springer-Verlag: Berlin, 1994; p 230.
(19) Geusic, M. E.; Morse, M. D.; O'Brien, S. C.; Smalley, R. E. *Rev. Sci. Instrm.* **1985**, *56*, 2123.
(20) Cotton, F. A.; Wilkinson, G. *Advanced Inorganic Chemistry*, 5th ed.; John Wiley & Sons: New York, 1988.
(21) Sievers, M. R.; Armentrout, P. B. *J. Phys. Chem.* **1995**, *99*, 8135.
(22) Meyer, F.; Armentrout, P. B. *Mol. Phys.* **1996**, *88*, 187.
(23) Andrews, M. P.; Mattar, S. M.; Ozin, G. A. *J. Phys. Chem.* **1986**, *90*, 1037.
(24) Kurikawa, T.; Nagao, S.; Miyajima, K.; Nakajima, A.; Kaya, K. Unpublished results.
(25) Nagao, S.; Miyajima, K.; Kurikawa, T.; Nakajima, A.; Kaya, K. Manuscript in preparation.
(26) Kurikawa, T.; Takeda, H.; Hirano, M.; Judai, K.; Arita, T.; Nagao, S.; Nakajima, A.; Kaya, K. Manuscript in preparation.